

Accumulated strain in low cycle fatigue of short carbon-fibre reinforced nylon 6

E. JINEN

Engineering College, Kyoto Institute of Technology, Matsugasaki Sakyo-ku, Kyoto 606, Japan

The deformation of short carbon-fibre reinforced nylon 6 (FRTP) which is induced by means of a low half-tensile-cycle fatigue test under a controlled loading system is examined. It has been found that the relation between the number of cycles and the total or accumulated strain is linear when plotted on a logarithmic scale, and empirical expressions for the two strains are presented. The dependence of the stress amplitude on the gradients of these plots was also found, and showed that the deformation process follows rate theory. The structural changes of the material in the process are discussed from the points of view of the stress dependence of the above two strains at the fracture, or the change with fatigue damage of the stress-strain relationship under monotonic tensile loading. The possibility is pointed out that the material lifetime can be predicted by measuring the accumulated strain arising from the deformation process.

1. Introduction

Recently, some possible explanations, theories and ideas have been proposed [1, 2] which are not limited in scope (such as those concerning fatigue or creep only) but which are unifying and deal with interdisciplinary problems for the estimation of fracture phenomena and prediction of the lifetime of materials. Regarding amorphous polymers, for example, ideas about the interpretation of the characteristic behaviour of materials under constant and cyclic loading have been proposed by Struik [3]. The reason for this trend seems to lie in the recognition that the damage to materials which are injured in service through accumulated damage effects is not caused by a single mode or factor, but arises from mixed damage due to multiple causes. So, not only in the estimation of lifetime in the field of material design but also in a broad sense for engineering design, it is necessary to point out that it is not possible to explain the result of the prediction by means of a single factor. Thus, in order to find a general law or derive a unified interpretation which is capable of explaining the fracture phenomenon, attempts have been made to cover not only the aspect that is related to practical demands, but also to adopt an academic approach using statistics or reaction rate theory, which are based on thermodynamics. It is not meaningless to apply such a general approach to the study of composite materials. Especially in the case in which the matrix is a polymer, the mechanical behaviour under the stress field shows a time dependence like that in viscoelasticity or viscoplasticity [4]. So, in the low cycle fatigue process of composites, it is safe to assume that the material deformation accumulates in all repeated cycles, so that in the phenomenon which is called the "low cycle fatigue" problem of aluminium alloys [5], cyclic strain-induced creep will be observed. In this

paper we deal experimentally with such questions concerning short carbon-fibre reinforced nylon 6 (FRTP), and we examine the contribution of accumulated deformation effects by repeated tensile stress, which is like a creep phenomenon in its relation to the lifetime of the material.

2. Experimental equipment, procedure and specimen details

2.1. Fatigue tests

An Instron type of machine (Shimadzu Autograph IS-10T) was used as a half-cycle tensile fatigue testing machine under load control. This test machine was equipped with an electronic ($X-T$) recorder and cycle counter for measuring the applied loads, which are controlled remotely by electric contact by setting microswitches and moving the pens of the recorder. The test specimen is clamped by chucks with a 130 mm span length and the gauge length is set up to 50 mm. The periods of load-deformation cycles for the stress levels 6.0, 6.5, 7.0, 7.5 and 8.0 kgf mm⁻² (1 kgf = 9.8 N) are 4.5, 5.6, 6.7, 7.9 and 9.3 sec per cycle, respectively. Thus, the magnitude of the strain rate in these repeated cycles corresponds to about 0.56, 0.58, 0.62, 0.65 and 0.67% sec⁻¹, respectively.

After setting the position of the microswitch for maximum load, tensile fatigue tests are done. In the mean time, the dynamic amplitude of the deformation and the points of maximum and minimum deformation are measured by reading the return points of the ball screw rotation of the machine on the following cycle numbers: 1, 3, 5, 7, 10, 15, 20, 50, 70 and 100 cycles. The measuring of these values in higher-number cycles is determined by the magnitude of the stress condition, and these measurements are continued until fracture of the specimen. The strain, the strain amplitude and the amount of the accumulated

deformation in the fatigue test are then calculated from these results. From these experiments, the relation between the damage to the material by the fatigue process and that arising from creep can be compared. The creep test is then conducted under the same stress conditions as for stress amplitude in the fatigue test, for specimens which were damaged for one half, one third and one quarter of the number of repeated cycles of the average life time. The temperature change of the specimen surface during the fatigue test is measured at frequent intervals with a thermistor thermometer which has a small flat pickup, because the matrix of the specimen is a thermoplastic resin and it is easy to suppose that there will be an increase in the temperature of the specimen. The hysteresis loop of the load-deformation relation in the fatigue process is also recorded by the test machine, and the areas of these loops are measured with a planimeter. Experiments were conducted in the following conditions: room temperature $20 \pm 2^\circ\text{C}$, relative humidity $60 \pm 5\%$.

2.2. Creep test

The test specimen is clamped at a distance of 130 mm, which is the same length as in the fatigue test condition, by two chucks and the gauge length is fixed at 50 mm with clip-on instruments. Measurements are performed with a travelling microscope. The instruments are arranged in a temperature-controlled box. The applied tensile stresses of the specimen are 6.0, 6.5 and 7.0 kgf mm^{-2} . The changes of the gauge length of the specimen are detected by the relative motion between the ferromagnetic core and the coil part of a linear differential transformer. The output signal from the transformer is converted by a rectifying circuit and input into a d.c. recorder. Recorded results are compared with the calibrated relation, and creep values are calculated at times of 1.5, 3, 6, 15, 21, 30, 42 sec and 1, 1.5, 2.5, 5, 10, 20, 40 min and 1, 2 h from the start of loading. The creep rupture test is also conducted in the same way as the creep test; the lifetime and the creep value at specimen failure are recorded. Both fatigue and creep tests were conducted at a room temperature of $20 \pm 1^\circ\text{C}$, $60 \pm 5\%$ relative humidity.

2.3. The test specimen

The test specimen is moulded to an ASTM A-type specimen with nylon 6 pellets (3 mm) which contain 15 wt % carbon fibre (7 to $8\text{ }\mu\text{m}$ diameter, Toray CM 1001 T 15) by an injection machine (Meiki SJ-35B); its configuration is shown in Fig. 1. The moulding conditions are as follows: temperature of the hopper part 210°C , middle 230°C , front part of cylinder 240°C , nozzle part 250°C , moulding pressure 720 kgf mm^{-2} , cycle 15 sec/15 sec, die temperature 80 to 90°C , screw revolution 100 r.p.m. Moulded specimens are tested after conditioning in a standard air-conditioned room for a year, and their moisture content seems to reach an equilibrium moisture condition (about 3.5%). Observed values are tensile elastic modulus $E = 578\text{ kgf mm}^{-2}$, tensile strength $\sigma_B = 9.1\text{ kgf mm}^{-2}$, proof stress $\sigma_{0.2} = 5.1\text{ kgf mm}^{-2}$ and elongation $\phi = 7.5\%$.

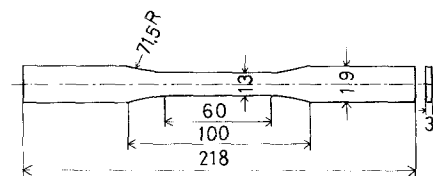


Figure 1 Specimen configuration. Dimensions in mm; R indicates radius of curvature.

3. Experimental results

3.1. The stress amplitude dependence of the fatigue life, dynamic creep and fracture strain

3.1.1. *S-N relation in low cycle fatigue*

As fundamental data for discussion of the problems in this study, and in order to estimate the degree of material damage by low cycle fatigue and to find the factors which have close relations to the fracture criteria of the fatigue life, the number of cycles to failure N is noted. It is commonly said, in the case of nonmetallic materials, that the $S-N$ relation shows some dependence on cyclic frequency. In this experiment, which deals with a specimen which is a reinforced composite of carbon fibres, the matrix is a thermoplastic resin. In order to set the rate of cyclic deformation it is therefore necessary to consider carefully the experimental conditions. The deformation speed which is possible in order to neglect a rising temperature of the specimen during repeated deformations (50 mm min^{-1}) is chosen as the crosshead speed of the fatigue experiment. The result of the $S-N$ relation under these test conditions is shown in Fig. 2. The plots for each stress level indicate the results for about ten specimens, and the short vertical lines denote the average values of the lifetime at each stress level. A noticeable result is that the scatter for the stress level 6.5 kgf mm^{-2} is wider than for the others, but the stress dependence of the lifetime for fatigue indicates a nearly linear relation except when the stress levels are 8.0 and 6.0 kgf mm^{-2} . These mean values of N are used as the expected lifetime and the scale of the material damage in creep rupture tests of fatigued specimens for discussion of the mixed damage effects of the material by fatigue and creep.

3.1.2. *Cyclic strain induced creep by low cycle fatigue*

In order to examine exactly the process of accumulating fatigue damage and the occurrence of fracture

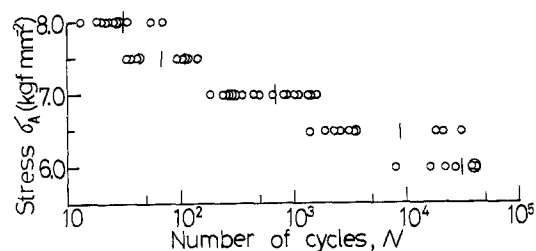


Figure 2 Stress against number of cycles; variation for short carbon-fibre reinforced nylon 6 under stress controlled by low cycle fatigue test. Vertical bars indicate the mean number of cycles of the experimental results.

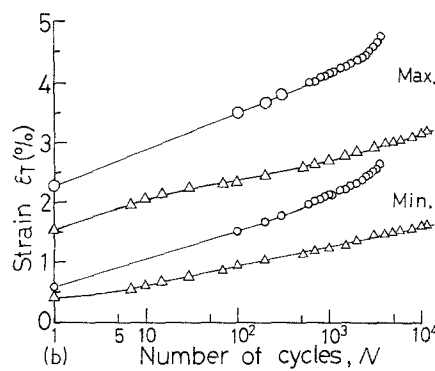
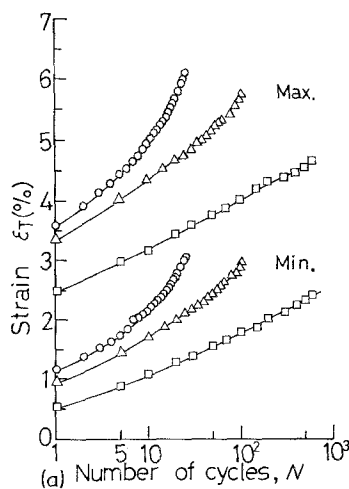


Figure 3 Strain against number of cycles. Max. and Min. indicate the total and accumulated strains during repeated cycles, respectively; the difference between Max. and Min. is the strain amplitude of the fatigue. (a) $\sigma_A = (\square) 7.0, (\Delta) 7.5, (O) 8.0 \text{ kgf mm}^{-2}$; (b) $\sigma_A = (\Delta) 6.0, (O) 6.5 \text{ kgf mm}^{-2}$.

phenomena, the induced deformation in every fatigue cycle is observed and the changes of these values in the fatigue process are converted into strain changes. The stress dependence of the strain changes by induced deformation for each stress level $\sigma_A = 8.0, 7.5, 7.0, 6.5$ and 6.0 kgf mm^{-2} are shown in Fig. 3. The marks Min. or Max. in these figures indicate the strain plot for which the applied stress is zero and the maximum value, respectively, for each given stress amplitude. This fatigue process is a half-tensile-cyclic one, so in spite of this process including the time when the applied stress is zero, it is easy to recognize that the deformation process in every repeated cycle increases with the number of cycles. That is, the plot for the changes of minimum strain at zero stress level shows a rising trend with increased numbers of repeated cycles. In other words, the deformation at the points where the stress reverses in each repeated fatigue cycle shifts to higher values, and the strain is accumulated. This is called "cyclic strain-induced creep" and is a dynamic creep phenomenon; a plot of Min. in Fig. 3 gives the dynamic creep curve. On the other hand, a plot of Max. traces the total strain values or the maximum ones in each repeated cycle [6, 7]. The difference between Max. and Min. then corresponds to the strain amplitude produced by applying a given stress. A general tendency of these relations may be recognized, in that the gradient and non-linearity of the Max. plot on a semi-logarithmic scale are usually larger than for the Min. ones, and there is some stress-dependence of this tendency.

Plots of the trace of the Max. and Min. values in Figs. 3a and b then separate into two groups, which are the differences between the total strain (ϵ_T) and the accumulated strain (ϵ_a) after repeated cycles at the given stress amplitudes, and these may be plotted on

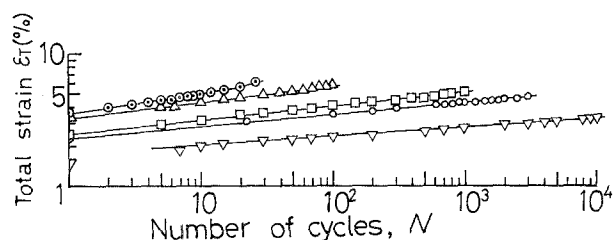


Figure 4 Log (total strain) against number of cycles: $\sigma_A = (\nabla) 6.0, (O) 6.5, (\square) 7.5, (\Delta) 7.5, (O) 8.0 \text{ kgf mm}^{-2}$.

log-log diagrams. The results are shown in Figs. 4 and 5 respectively. It is obvious that there are linear relationships in changes of both the total and the accumulated strains, except in the early stage of the fatigue process, and a stress-dependence is found in the relation between the magnitude of the gradient and the stress amplitude. In addition, there is a range of values for the fracture strain at the final stage of the fracture process. That is, the total strain values near the fracture point increase to the same extent with an increase in the stress amplitude; however, the accumulated strain values fall in a narrower band than the total strain. This result suggests the character of the material deformation or the existence of a criterion for the fracture phenomenon [8, 9].

3.1.3. The stress-amplitude dependence of the changes in total and accumulated strains

As shown in Fig. 3, a good linear relationship between the two kinds of numbers of repeated cycles are found. The stress-amplitude dependence must therefore be checked. In Figs. 6 and 7 the stress amplitude is plotted against the average value of the gradient, $S' = d(\log \epsilon_T \text{ or } \log \epsilon_a)/d(\log N)$, for about ten specimens taken from the results of Fig. 3. The results show a linear relationship. Moreover, it is found that there are limitations in the stress amplitude which produce a cessation of the increase in both the changes of the total and accumulated strains. That is, the values on the stress amplitude axis where the strain change is zero are found by extrapolation of the experimental lines in Figs. 6 and 7. These values are 4.4 and 5.2 kgf mm^{-2} , for zero change in ϵ_T and ϵ_a respectively.

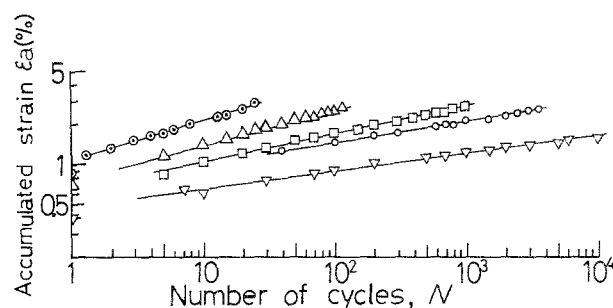


Figure 5 Log (accumulated strain) against number of cycles: $\sigma_A = (\nabla) 6.0, (O) 6.5, (\square) 7.0, (\Delta) 7.5, (O) 8.0 \text{ kgf mm}^{-2}$.

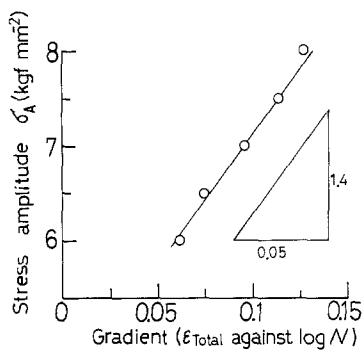


Figure 6 The stress-amplitude dependence of the gradient for the relation between the total strain and the number of cycles.

3.1.4. An experimental formula for the deformation

From the results in the previous section, it is possible to express the relationship between the total or accumulated strains and number of cycles by a simple exponential expression like the one shown below:

$$\log(\varepsilon_T \text{ or } \varepsilon_a) = \left(\frac{\sigma_A - \beta}{\alpha} \right) \log N$$

that is,

$$\varepsilon_T \text{ or } \varepsilon_a = N^{\frac{\sigma_A - \beta}{\alpha}}$$

where ε_T or ε_a is the total or accumulated strain, σ_A is stress amplitude, N is the number of cycles and α and β are constant; their values for the total strain or accumulated ones are 28 and 4.4 or 8.3 and 5.2 using the assigned units, respectively.

3.1.5. The strain-amplitude dependence of strain-amplitude range (ε_R)

As mentioned in Section 2, this fatigue test is a half-cycle tensile one and has been conducted using constant load or stress control. As is well known, even for metallic materials in the case of a low cycle fatigue by this method, the strain-amplitude range shift to a higher level is gradual. It is therefore easy to understand the results of Figs. 3 to 5. In this case, the strain amplitude range is the difference of the strain between the total and accumulated ones in each cycle. Fig. 8 shows the stress dependence of the strain amplitude range throughout all the fatigue process. The vertical bars indicate the value of the strain amplitude under the given stress levels at the half-life cycles of the mean life (\bar{N}), and the left and right sides of the horizontal bar indicate the values at the beginning and near the final cycle of the process, respectively. The stress-

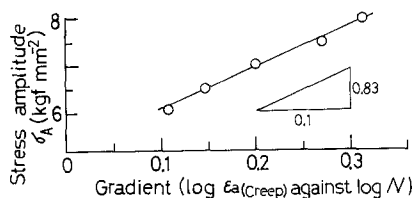


Figure 7 The stress-amplitude dependence of the gradient for the relation between accumulated strain and the number of cycles.

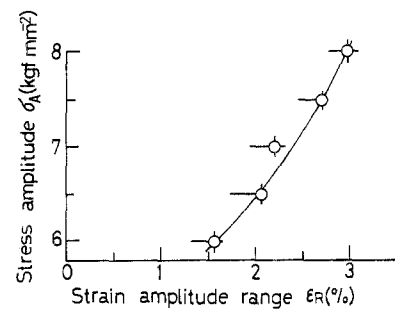


Figure 8 The stress-amplitude dependence of the strain amplitude range. Vertical and horizontal bars indicate the strain amplitude at the half cycle of the mean life and the strain range in all fatigue processes, respectively.

strain relationship of the first cycle and the final stage of the fatigue process must therefore be checked, and they correspond to the end of the left or right side of the horizontal bar, respectively. At the beginning, it is noteworthy that the stress dependence of the strain amplitude for the first cycle shows a near-linear relation, except when the stress amplitude is 7.0 kgf mm^{-2} . In regards to the stress dependence of the amplitude range at the half-life cycle of the mean life, however, the relation changes to a non-linear one. Moreover, the values of these strain ranges for each given stress amplitude exist in the final stage of the whole process. These results seem to show the character of the relation between the deformation and accumulated fatigue damage effect of the material. If it is assumed that such a tendency for a non-linear relationship continues to hold in the lower stress-amplitude range, it is found by extrapolation of the curve that the stress level at which the change of the strain amplitude range disappears is about $\sigma_A = 4.65 \text{ kgf mm}^{-2}$. It is of interest that this value nearly agrees with the extrapolated value of the relationship derived from Fig. 6.

3.1.6. The stress-amplitude dependence of the fracture strain

In the case of dispersed short-fibre reinforced composites, the fracture strain relates to the stress-field condition and to structural parameters of the material, such as the mean fibre length, fibre content and fibre orientation, or the adhesive state at the interface between the surface of the fibre and the matrix. From

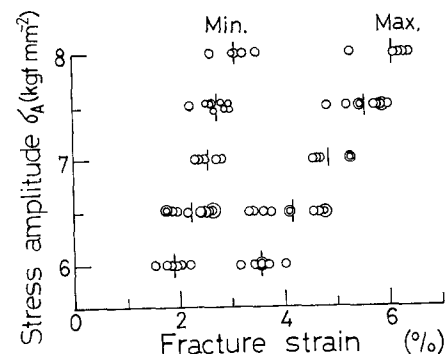


Figure 9 The stress amplitude dependence of the total (Max.) and accumulated strain (Min.) near to the fracture of the specimen. Vertical bars indicate the mean value of each strain.

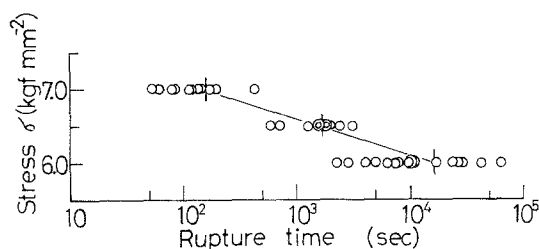


Figure 10 The creep rupture time variation of short carbon-fibre reinforced nylon 6. Vertical bars indicate the mean values of the rupture time.

such a point of view, it is necessary to examine the stress-dependence of the limiting strain in the final stage of the process. Fig. 9 shows these results for accumulated and total strain for Min. and Max. data respectively. The vertical bars indicate the mean values of these strains. The result that there is a stress-amplitude dependence of these strains is obvious, and it is noticeable that the dependence for accumulated strain shows less sensitivity than that for the total strain, and a near-linear relationship.

3.2. The tensile creep test

In order to discuss the difference between the damage effects by fatigue and creep under the same stress conditions, and to identify clearly the creep properties, tests for accumulated damage by fatigue and the creep test have been conducted for stress levels $\sigma = 6.0, 6.5$ and 7.0 kgf mm^{-2} .

3.2.1. The stress-dependence of the rupture time

Fig. 10 shows the distribution of plots for the creep rupture time (sec), and the vertical bars indicate the mean values of these results. The standard deviations of the rupture time for the stress levels $\sigma = 6.0, 6.5$ and 7.0 kgf mm^{-2} are 4.20, 2.85 and 1.86 on the logarithmic scale, respectively. By drawing a straight line through the mean values for each given stress, the relationship is seen to be a near-linear one. As has been shown in Fig. 2, this is the same tendency which was obtained from the results of the fatigue test, which indicated that the scatter had a near-linear relationship with the exception of the result for $\sigma_A = 8.0 \text{ kgf mm}^{-2}$.

3.2.2. The static creep property

As shown in Fig. 11, the creep property is described by a linear relationship by using a double logarithmic plot, except when the maximum stress level is $\sigma = 7.0 \text{ kgf mm}^{-2}$ and the gradient of these lines seems to

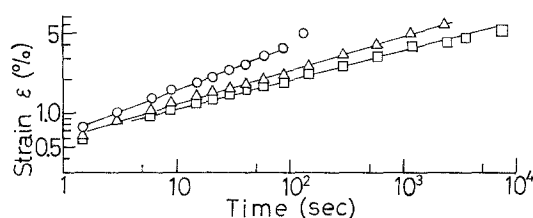


Figure 11 Log (creep strain) against time. $\sigma = (\square) 6.5, (\circ) 7.0 \text{ kgf mm}^{-2}$.

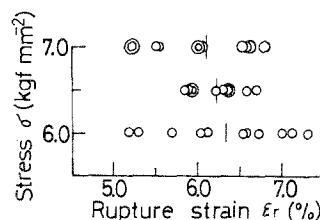


Figure 12 The stress dependence of the rupture strain. Vertical bars indicate the mean values.

exhibit stress-dependence. Moreover, it is notable that the strain at the final stage of the creep process indicates nearly the same rupture strain, that is about 6.5%.

3.2.3. The rupture strain

Fig. 12 shows the rupture strain, and the vertical bars indicate the mean values of these results for the given stress levels. The mean values of the strain gradually increase with a decrease of the stress level, so the stress dependence indicates a loosely negative relation. This result is opposite to the one for the fatigue test, and notable because it seems to imply a difference between the damage effects on the material by the fatigue and creep processes.

3.3. The accumulated damage effect in the fatigue process

3.3.1. The stress-strain relationship

At first, in order to recognize the accumulated damage effects and the changes in the mechanical properties during a repeated tensile cycle, and to compare the mechanical behaviour under a monotonic increasing load with a repeated tensile fatigue system, the stress or the stress amplitude of the first cycle and the strain relationship is observed; these results are shown in Fig. 13a. In this figure, the curved line indicates the relationship of the monotonic increasing load system for the virgin specimen, and the circles denote the first cycle in the fatigue process under the given stress levels. The later relationship shows a nearly linear one which corresponds to the trace for the left side of the horizontal bars in Fig. 8. Obviously, this relationship exists in the inner side of the static stress-strain relation so the fatigue cycles are performed at lower stress levels for the same strain level, when compared with the monotonic increasing load system. By comparison of this line with the result in Fig. 8, it is found that the curve shifts to the right side of the strain axis according to the progress of the fatigue process. Furthermore, the rising part of the static curve does not show an exactly linear relationship, and on the whole, the shape of the curved line is typical of other FRP.

Fig. 13b shows for comparison the static curve for the virgin specimen (solid line) and the fatigued specimens which have been damaged by fatigue under the stress amplitude $\sigma_A = 6.5 \text{ kgf mm}^{-2}$ for one-third (indicated by the dotted line and circles) or one-half (chain line and crosses) of the mean number of life cycles. This result shows the change in the mechanical behaviour caused by fatigue, that is, the following changes are recognized: that the linearity of the rising

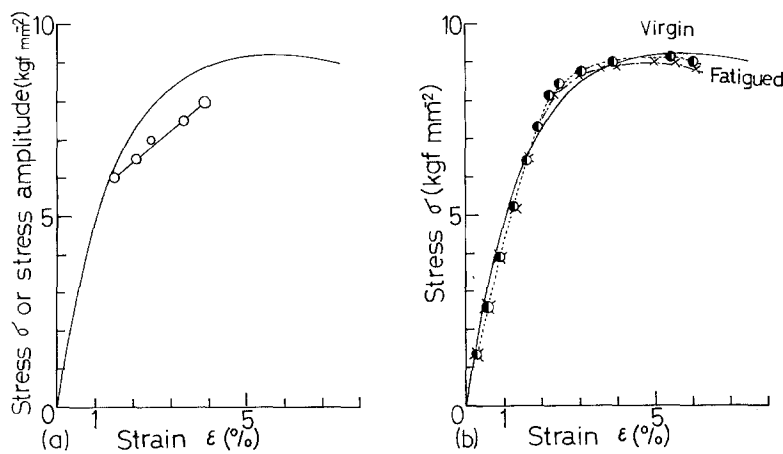


Figure 13 (a) Comparison of the stress-strain relation by monotonic increasing tensile test (solid line) and for the first cycle in the fatigue process (circles). (b) The change of the stress-strain relation by fatigue damage. The solid line is for the virgin specimen ($n = 0$); circles and crosses denote the results for fatigued specimens for one-third or one-half of the mean life cycle numbers, respectively. $\sigma_A = 6.5 \text{ kgf mm}^{-2}$.

portion the curve improves and the curvature in the middle part (which corresponds to the portion between the elastic increase and the region for plastic deformation) decreases with an increase in the number of cycles; moreover, a decrease in the fracture strain is found. The reason for these changes seems to be a decrease of the non-linearity in the early stage of the deformation; in other words, in this region the rigidity of the specimen increases in some degree by changes of the rheological condition in the region of the interface between the fibre and the matrix. On the other hand, the reasons for the later changes are debonding of the interface and/or the breaking of fibres. On the whole, the stress-strain relationship for the fatigued specimen changes or approaches the pattern of an ideal elastic-plastic material.

3.3.2. The change of the strain energy in the fatigue process

As is well known, the loop area which is described by the load-displacement relationship with repeated cycles in the fatigue process gives the strain energy. So, in order to discuss structural changes during the process, it is important to examine the parameter changes due to the change of the mechanical properties of the material, such as increasing the strain by softening or decreasing it by increasing the stiffness. This result for the stress amplitude $\sigma_A = 6.0 \text{ kgf mm}^{-2}$ is shown in Fig. 14. Obviously, there are three stages in this process: an increasing stage in the transient region, an equilibrium stage, and an increasingly rising stage near the end of the process.

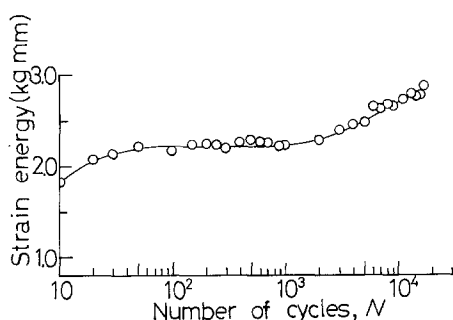


Figure 14 The changing of strain energy in the fatigue process, for $\sigma_A = 6.0 \text{ kgf mm}^{-2}$.

3.4. The observation of the fracture surface after the fatigue or creep rupture

Though the main aim of this study is to make clear the relation between the deformation in the process of low cycle fatigue and the mechanical condition, observation of the fracture surface of the specimen is interesting and useful for the consideration of the mechanism of material deformation. Figs. 15 and 16 show scanning electron microscope (SEM) photographs of the stable crack-propagation area after low cycle fatigue and creep rupture respectively, under the same stress conditions (σ_A , $\sigma = 7.0 \text{ kgf mm}^{-2}$). The number of cycles to fracture in the fatigue case and the rupture time in the creep sample are $N = 987$ cycles and 1750 sec respectively. After the fracture of the specimen it is easy to recognize many holes as in a honey-comb, which have been formed by pulling out short fibres from the opposite fragment of the specimen, or standing fibres which have been pulled out from the matrix resin of the other fragment; this is a notable point for consideration of the deformation process. Moreover, the fibre orientation of the specimen (which relates closely to its mechanical properties) and the behaviour of the deformation is estimated by observation of the distribution in orientation of the standing fibres. From this point of view, SEM examination of the fracture surface of both fragments of the specimen is performed. It is then found that the fibres mainly orient parallel to the longitudinal direction of the specimen. This direction accords with the loading direction, and is perpendicular to the photographs which are shown in Figs. 15 and 16.

At first sight, the characteristic features of these fracture surfaces due to the different loading systems applied to the material seem to be indistinguishable in the two photographs. Higher magnifications of Figs. 15a and 16a are shown in Figs. 15b and 16b, respectively. The difference between the characteristic features of these fracture surfaces seems to be in the area of the matrix. That is, a significant ductile-fracture phenomenon like a resin flow is easily recognized around the hole of the fracture process, rather than in the creep rupture area. Moreover, a larger gap between the fibre and the matrix is seen in all the holes of the fracture surface. This phenomenon seems to be due to the repeated deformation effect of the fatigue process, because these photographs show the situation

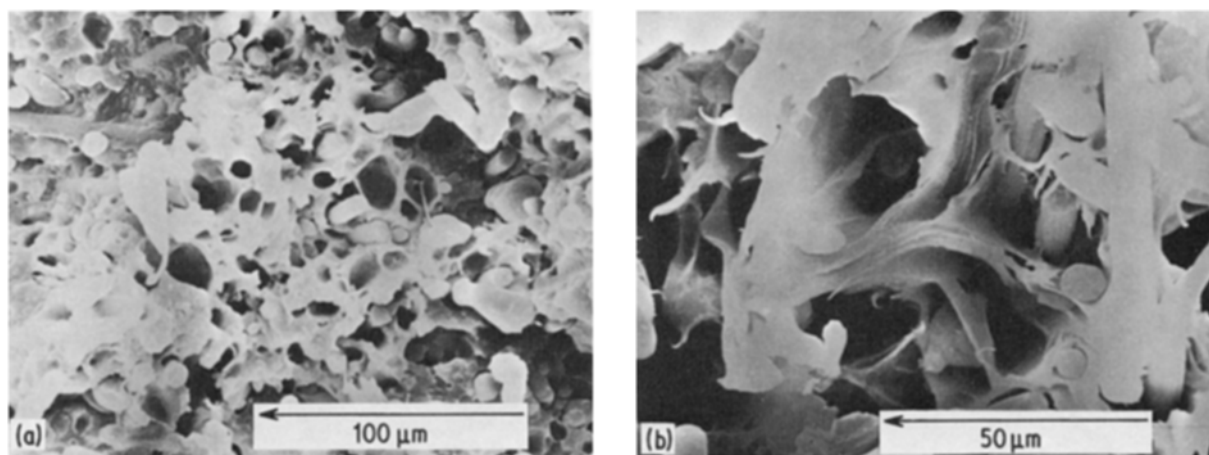


Figure 15 Scanning electron micrographs of the fracture surfaces in the stable crack propagation area, using the low cycle fatigue process. Stress amplitude $\sigma_A = 7.0 \text{ kgfmm}^{-2}$, number of cycles to fracture $N = 987$. Scale arrow also indicates direction of crack propagation.

in which the area of stable crack growth occurs. The other noticeable difference between the figures is shown in the case of creep rupture (Fig. 16b). Many fibroid resins, which tie in the gap between the carbon fibre and the surface of the resin hole, are found everywhere. The existence of these fibroid ties influences the mechanical behaviour of the creep phenomena of the material.

4. Discussion

As shown in Figs. 4 and 5, the mechanical behaviour for the changes of the total or accumulated strain by repeated cyclic loading can be expressed by a linear relationship on a logarithmic scale. The characteristic feature of this result implies that the phenomenon is governed by a rate process, and this fact is an essential point for understanding the fatigue process as a whole. This result, as is well known, shows the same tendency as that for the response of the deformation of metallic alloys by a low cycle fatigue test. The strain amplitude for different loading cycles in the process seems to have a nearly constant value, because in all repeated deformation cycles the difference between the total strain and the accumulated strain corresponds to the strain amplitude of each cycle. So, in spite of the fact that this specimen is moulded with

pellets, which used thermoplastic resin as the matrix, it is considered that there is little change in the mechanical properties for rheological reasons, such as an increase of temperature during the fatigue process; the deformation speed and the frequency of the test constitute very slow-speed conditions. Therefore, the reason for the changing tendency of the accumulated strain seems to be related to the process of structural changes such as the debonding, slipping and pulling out of the fibres, and to an extension of the crack. This process progresses to nearly the final state of the fracture while keeping the same relationship. The cause of the change of this phenomenon in the process therefore seems to be mainly a uniprocess governed by the rate process. From the macroscopic standpoint, this phenomenon is the accumulation of the plastic deformation due to a cyclic load; however, it must be considered from the microscopic viewpoint to clear up the relationship between the change of the property and also the structural changes in the material.

The specimen used in this experiment, as described in Section 2, was moulded by injection from one end. As shown in Section 3.4, the main direction of dispersed fibre orientation seems to be in accord with the loading direction. At this stage, debonding by the

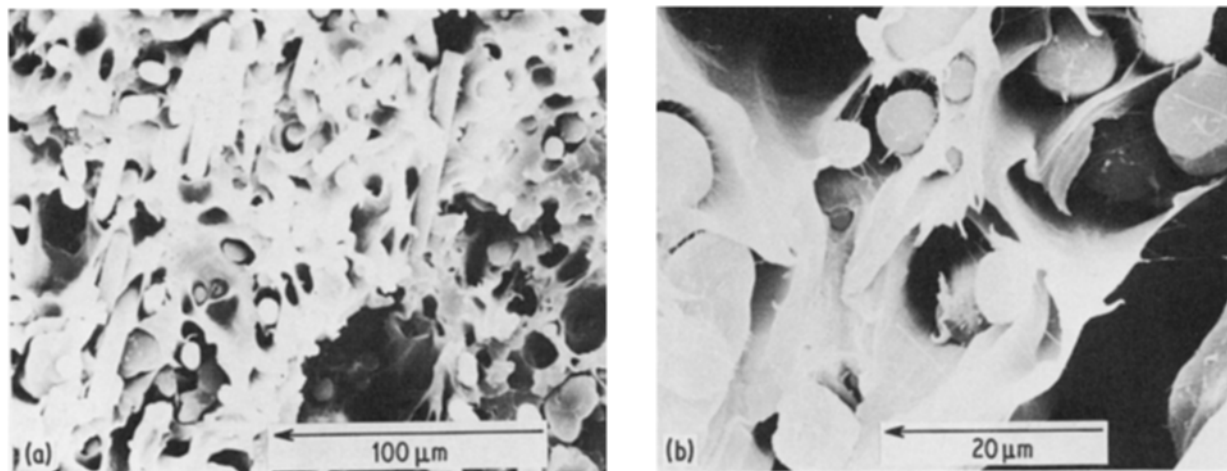


Figure 16 Scanning electron micrographs of the failure surfaces in the stable crack propagation area, using the creep process under a stress amplitude of $\sigma = 7.0 \text{ kgfmm}^{-2}$. The time from the rupture to the failure is 1759 sec. Scale arrow also indicates direction of crack propagation.

maximum tensile stress does not occur at the interface between the fibre and the matrix but takes place at both ends of it, so it seems that these points are most susceptible to damage; the phenomenon of debonding will begin at these points, while endurance to repeated loadings is shared by the fibre and the matrix. For this reason, though some fibres may be broken in the process of mould injection, since the mean fibre length of the specimen is half the value of the pellet length (about 3 mm) [10], a large aspect ratio will be expected because the fibre length is much longer than its diameter (7 to 8 μm). Moreover, the ratio of the fibre strength to that of the matrix is very large. Therefore, the reason for the phenomena which have been shown in Figs. 3 and 4 seems to be concerned with the debonding process between the fibre and matrix rather than the breaking of fibres during a repeated deformation process. The other result in support of this conclusion can be found in Fig. 3a: in the case of the higher stress levels, the tendency of the plot of the relationship between the number of cycles and the total strain deviates from the linear relation towards the final stage of the process. The reason for this tendency must be thought to be in the progression of significant structural changes, such as the breaking of fibres and the joining of local debonded parts, rather than in a local debonding process.

As shown in Fig. 9, the other phenomenon which has a close relation to such progressive and continuous structural changes in the material is the stress-amplitude dependence of accumulated strain or the total strain when the specimen fractures. The stress-amplitude dependence of accumulated strain indicates a very weak, nearly linear relationship; however, in the case of the total strain it is very strong and the ratio of the gradients is about 2.3. The total strain is a parameter which can show a change of property by the effect of repeated deformation. The evidence which supports this point can be found in Fig. 15b; that is, as described in Section 3.4, the differences in the stable cracks which extend the area due to the fatigue process from one side by creep rupture. These are easily recognized in a notable flowing deformation of the matrix, or in the size of the gap between the fibre and the hole wall. On the other hand, the stress-dependence of the rupture strain by a static creep process, which is a uniprocess as shown in Fig. 12, is almost indiscernible. So, by decreasing the stress level with a slight increase in the strain, the results indicate quite a different tendency in the case of the fatigue process which involves a repeated deformation effect. From these results, therefore, in the case of the process with a low stress amplitude, it seems that the contribution to the decrease of the fracture strain is due more to the shortening of the mean fibre length by damage at a weak bonding site following repeated deformation with a high number of cycles, rather than to the pull-out effect [11, 12] due to debonding between the fibre and the matrix.

As another example which is related to the above discussion, the comparison of results from a monotonic tensile test for the fatigued specimen with those from the virgin one is shown in Fig. 13b. The stress-

strain curve for the former indicates a tendency towards a decrease in fracture strain and tensile strength as a consequence of fatigue damage, which decreases with a decrease in the progress of the process. This tendency also accords with the results and supports the above discussion. This therefore supports the existence of a common factor which relates the accumulation of the deformation by fatigue and the structural change by the creep process, and these factors have a weak dependence on the stress amplitude rather than on the total strain. In order to examine the character of the accumulated strain from another point of view, the stress-amplitude dependence of the gradient for the relation between the strain and the relative ratio n/\bar{N} (where n and \bar{N} are arbitrary numbers and the mean number of cycles for the life, respectively) is shown in Fig. 17; the dotted lines show the stress dependence for the static creep process. It is notable that both relationships are linear, and when the slope of the two lines is compared it is interesting that the gradient in the fatigue process is about twice that of the creep process. Moreover the stress intercepts for zero gradient, $d(\log \epsilon_a)/d(\log t)$ or $d(\log \epsilon_a)/d(\log n)$ (i.e. the zero creep rate) for the dynamic and static cases, are 5.3 and 4.8 kgf mm^{-2} for the fatigue and creep processes respectively. These values imply the existence of an inner stress. In the case of FRTP, as is well known, the dynamic inner equilibrium is frozen or fixed in the cooling stage of the injection process. It is therefore easy to suppose that the material has an inner stress, even under stress-free conditions. Of course, this stress is not constant and it changes under given surrounding conditions such as temperature or humidity. In the case of this specimen, the material of the matrix swells upon absorption of moisture. If, during conditioning of the specimen, about a 0.2% change of the longitudinal dimension occurs due to moisture absorption, then by using an estimate from the stress-strain curve (Fig. 13) a resultant stress of about 1 kgf mm^{-2} can be obtained. This estimate for the deformation is an approximation. Previously, the author dealt with a similar problem for a glass-fibre reinforced nylon 6 [13].

There is the same problem in dealing with the estimation of the variation of the relative ratio n/\bar{N} for

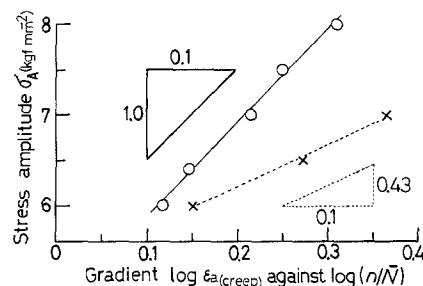


Figure 17 Solid lines show the stress-amplitude dependence of the gradient for the relation of \log (accumulated strain) against \log (relative fraction n/\bar{N}), where n and \bar{N} are arbitrary and mean values of the cycle number, respectively. Dotted lines show the same relation for the creep process; the horizontal axis then indicates the gradient for the relation of \log (creep strain) against \log (relative fraction t/\bar{T}), instead of n/\bar{N} in the fatigue process, where t and \bar{T} are arbitrary time and the mean value of the rupture time.

fatigue with t/\bar{T} for the creep process, and a need for more discussion. But, as pointed out, the possibility of estimating the remaining life of a material in the low cycle fatigue process by measuring the accumulated strain has been established.

5. Conclusions

The deformation of a dispersed short carbon-fibre reinforced nylon 6, arising from the half-cycle tensile system of low cycle fatigue (stress amplitude $\sigma_A = 6.0$ to 8.0 kgf mm^{-2}), was examined from various points of view concerning the relationship between the damage effects on the material. The deformation behaviour of the material in the fatigue process is represented by a linear relationship on logarithmic scales for the number of cycles and the strain; the deformation also increases with an increase in the number of repeated cycles. Therefore, the strain level at the minimum point of the deformation by cyclic loading shifts to higher values with an increase in the number of cycles, and a strain-accumulation phenomenon which is similar to that observed with an aluminium alloy or other metals has been observed. The accumulated deformation value which corresponds to the dynamic creep value is converted into the strain and examined. The same linear relationship on a logarithmic scale was observed for the total strain and the number of cycles, and a linear stress-amplitude dependence obtained. Hence the deformation process of the material is a phenomenon which is ruled by a rate process. The magnitudes of the slopes of the two lines which express the stress-amplitude dependence of the total and accumulated strains in the fatigue process are 28 and 8.3 by unit of kgf mm^{-2} , respectively.

In order to examine the character of the accumulated strain in the fatigue process and make a comparison with the static creep strain under the same stress conditions ($\sigma = 6.0, 6.5$ and 7.0 kgf mm^{-2}) as for the case of fatigue, the stress dependence of the relation between the accumulated strain and the ratio of n/\bar{N} , or that for the creep strain and the ratio t/\bar{T} , or that for the creep strain and the ratio t/\bar{T} , are compared with each other. (Here n or t are arbitrary values for the number of cycles or the time, while \bar{N} or \bar{T} are the number of the mean life cycles and the mean life time.) It has then been found that the contribution to the material deformation by repeated effects in the fatigue process is about twice as large as for static creep. Moreover, the damaging effect on the material by fatigue is examined from the points of view of the

stress-amplitude dependence of the fracture or accumulated strain and of the strain amplitude, and these have been compared with the results for the creep process. The structural change of the material with fatigue is also estimated and discussed by comparison of the stress-strain relationship for the fatigued specimen with that of the virgin sample, and the change of the strain energy during the process by cyclic deformation. From the above discussion and some consideration of the deformation in the fatigue process, it has been pointed out that there is a possibility of estimating the life of a material by measuring the accumulated strain.

Acknowledgements

The author wishes to thank Junichi Matsui and Sadao Arai of Toray Co. Ltd for supplying pellets and providing for the injection of the specimen, and Yoshiyuki Mineoka for assisting in a part of this work. The author also thanks Professor Megumu Suzuki of Kyoto Institute of Technology for encouragement, and Dr Peter W. R. Beaumont of the Department of Engineering, University of Cambridge for sending useful reprints of his work. This work was supported in part by a Grant-in-Aid for Science and Research from the Ministry of Education, Japan.

References

1. T. YOKOBORI, "Strength, Fracture and Fatigue of Materials" (Wolters-Noordhoff, Groningen, 1965).
2. *Idem*, "An Interdisciplinary Approach to Fracture and Strength of Solids" (Wolters-Noordhoff, Groningen, 1968).
3. L. C. E. STRUIK, "Physical Ageing in Amorphous Polymer and other Materials" (Elsevier, Amsterdam, 1978).
4. E. JINEN and M. SUZUKI, *J. High Polym. Jpn.* **30** (1973) 504.
5. L. F. COFFIN, *Trans. ASME, Ser. D* **82-4** (1966) 671.
6. M. J. MINDEL and N. BROWN, *J. Mater. Sci.* **9** (1974) 1661.
7. J. W. TEH, J. R. WHITE and E. H. ANDREWS, *ibid.* **10** (1975) 1626.
8. P. W. R. BEAUMONT and P. D. ANSTICE, *ibid.* **15** (1980) 2619.
9. J. K. WELLS and P. W. R. BEAUMONT, *ibid.* **17** (1982) 398.
10. E. JINEN, M. SUZUKI, M. NAGATA and M. NAKANURA, *J. High Polym. Jpn.* **27** (1970) 689.
11. P. LAWRENCE, *J. Mater. Sci.* **7** (1972) 1.
12. O. BØCKER PEDERSEN, *ibid.* **9** (1974) 948.
13. E. JINEN, *J. High Polym. Jpn.* **33** (1976) 489.

Received 30 July 1984

and accepted 28 February 1985